Published by :
http://www.ijert.org

International Journal of Engineering Research & Technology (IJERT)
ISSN: 2278-0181
Vol. 6 Issue 09, September - 2017

3-D Finite Element Analyses of Diaphragm Wall Displacements in Cohesionless Soil

Bahr, M.A.
Professor,
Department of Civil Engineering,
Al-Azhar University
Cairo, Egypt

Hassan, A.A.
Professor,
Department of Civil Engineering,
Al-Azhar University
Cairo, Egypt

Tarek, M.F.
Professor,
Department of Civil Engineering,
Al-Azhar University
Cairo, Egypt

Hemeida, A.M.
Ph.D. Student,
Department of Civil Engineering,
Al-Azhar University
Cairo, Egypt

***Abstract*— The demand for underground space, for use as transport tunnels, parking garages and storage spaces, in many heavily urbanized areas requires the construction of deep excavations in close proximity to sensitive structures. In these situations, accurate predictions of the wall and ground movements are important design criteria in order to avoid damage to adjacent structures. Therefore, a 3D numerical analysis can be valuable to assess the performance of the earth-retaining structure and the surrounding soil. The principal aim of this paper is to study the combined influence of the geometric configurations and the properties of the cohesionless soil on behavior of the diaphragm walls and surrounding soil under static and seismic conditions. In this regard, a 3D numerical analysis is carried out for different configurations of deep excavation in cohesionless soil supported by diaphragm wall. The results show the main impacts of the investigated parameters on the behavior of the earth-retaining structure under static and seismic conditions.**

I. INTRODUCTION

Construction of deep excavations in urban environments often raises significant concerns related to induced ground movements and potential damage to adjacent buildings. Therefore, it is critically important to estimate and control the magnitude and distribution of ground movements that result from developing underground space. One of the widespread in-situ walls is the diaphragm wall which provides structural support and water tightness. It is the most proper technique for many deep excavation projects, large civil engineering works, underground car parks, and metro tunnels. The general magnitude and pattern of ground deformations adjacent to supported excavations was first practically proposed by Peck [1] who suggested that the deformation behavior was mainly dependent upon the ground type through which the excavation was made. Soil type is a key factor since the behaviour of deep excavations is governed by the interaction between the soil and the retaining wall. In general, larger wall and ground deformations are induced due to excavations in soils with lower strength and stiffness. This aspect is further studied by other researchers (e.g., Goldberg et al. [2]; Clough & O'Rourke [3]) who examined monitored data of deep excavation sites and correlated it to the subsoil conditions.

Law et al. [4] investigated numerically the influence of the excavation corner on the performance of a diaphragm wall in Malaysia. The results demonstrated that corner effect has decreased the induced wall deformations. Similar finding is reached by Ahmad et al' [5] who studied the three-dimensional performance for one of Greater Cairo underground metro stations (Rod El-Farag Station), and reported that the behavior of deep supported excavations should be ideally investigated as a three-dimensional problem. Wood [6] analyzed the dynamic response of homogeneous linear elastic soil trapped in between two rigid walls connected to a rigid base, providing an analytical solution. Kitsis et al. [7] studied the seismic response of concrete walls retaining noncohesive backfill. It was found that in the the design of massive and rigid earth retaining walls, it is reasonable and warranted to assume a synchronous action of the the maximum values of wall inertia and seismic earth thrust.

This research investigates numerically the combined effect of varying the geometric configurations of deep excavations and the properties of the cohesionless soil on the behavior of diaphragm wall and surrounding soil under static and seismic conditions.

II. MODELLED DEEP EXCAVATION

The height of final excavation level (H) is taken as 10 m, 15 m, and 20 m and total width of the excavation (B) is 20 m. Different cases of length over width of the excavation dimensions on plan are considered as follow: L/B = 1, L/B = 3, and L/B = 5. Two cohesionless soil deposits are considered, dense and loose to medium dense sands. The ground water level is at 3 m depth from the natural ground surface. All the above mentioned parameters are investigated under static and seismic conditions. The 3-dimensional finite element program PLAXIS (AE version) is adopted in this study with the Hardening Soil model. To perform finite element calculations, the geometry has to be divided into elements. A composition of finite elements is called finite element mesh. PLAXIS 3D Program allows for a fully automatic generation of finite element meshes. Figure (1) illustrates the 3D mesh layout of the proposed finite element model.

International Journal of Engineering Research & Technology (IJERT)
ISSN: 2278-0181
Vol. 6 Issue 09, September - 2017

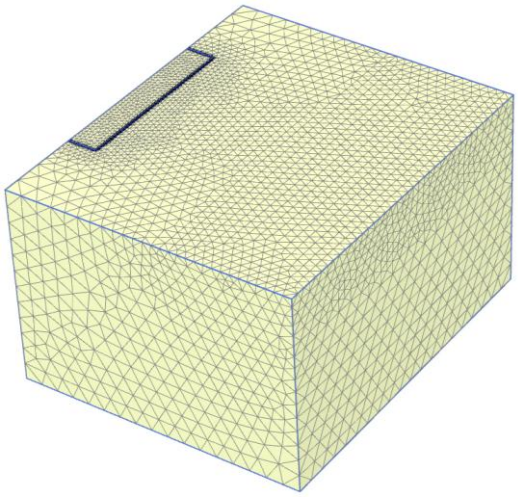

Fig. 1. 3D mesh layout of the proposed finite element model

A. Case of Excavation Height (H = 15 m)

Figure (2) shows plan of the excavation site for the proposed study, while Figure (3) shows the cross section of case (H = 15 m). Four rows of struts are used. The parameters of the proposed soil deposits are presented in Table (1). E_{50} is set equal to E_{oed}, and E_{ur}/E_{50} = 3 (Brinkgreve et al' [8]). Different cases of length over width of the excavation dimensions on plan are adopted: L/B = 1, L/B = 3, and L/B = 5. For the seismic condition, the considered values of Peak Ground Acceleration (PGA) are in range of 0.1g to 0.3g.

It should be noted that the loose sand deposit has fines content of approx. 15%, and since the fines content decreases the liquefaction potential (Seed et al' [9]), and due to that the relative density of the cohesionless soil is increasing with depth owing to the increased overburden pressure, liquefaction is not likely to happen for peak ground accelerations ranging between 0.1g and 0.2g. However, for PGA=0.3g, the loose sand deposit has high liquefaction potential, and accordingly mitigation measures shall be taken.

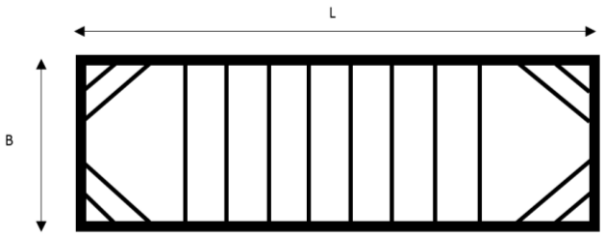

Fig. 2. Plan of the excavation site for the proposed study

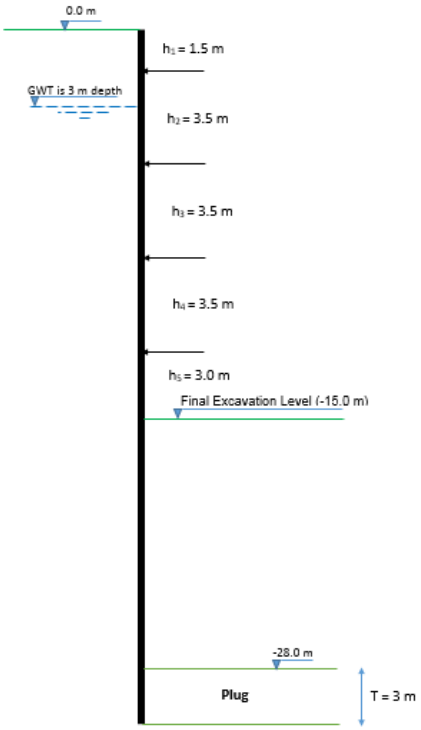

Fig. 3. Cross section of the considered deep excavation system (Excavation Height = 15 m)

Table 1. Parameters of the cohesionless soil deposits adopted in the current study

Sand State	ϕ (degrees)	E (MPa)	Dry Unit Weight (kN/m^3)
Dense	38	112.5	18
Loose	31	17.5	14

A.1 For Length Over Width Ratio of the Excavation Dimensions on Plan (L/B = 1)

Figure (4) and Figure (5) present the wall displacement profiles under static and seismic conditions for length over width ratio (L/B = 1) of the excavation dimensions on plan. Figure (4) has a series of profiles showing the wall displacements of dense sand under static condition against range of wall displacements expected to occur under different seismic conditions (PGA=0.1 to 0.3g). Furthermore, Figure (5) has a series of profiles showing the wall displacements of loose sand under static condition against range of wall displacements expected to occur under different seismic conditions (PGA=0.1 to 0.3g). At the static condition, the maximum lateral displacements of the wall are approximately ranging between 0.0119 m and 0.0287 m for dense and loose sands. However, at the seismic condition, the maximum wall lateral displacements are within 0.0163 m and 0.1085 m for peak ground acceleration (PGA) oscillating between 0.1 and 0.3g.

It should be noted that the maximum wall lateral displacements for the static condition occur at a depth of approximately 13 to 15 m below ground surface, while its location is at depth of 14 to 19.6 for the seismic condition.

International Journal of Engineering Research & Technology (IJERT)
ISSN: 2278-0181
Vol. 6 Issue 09, September - 2017

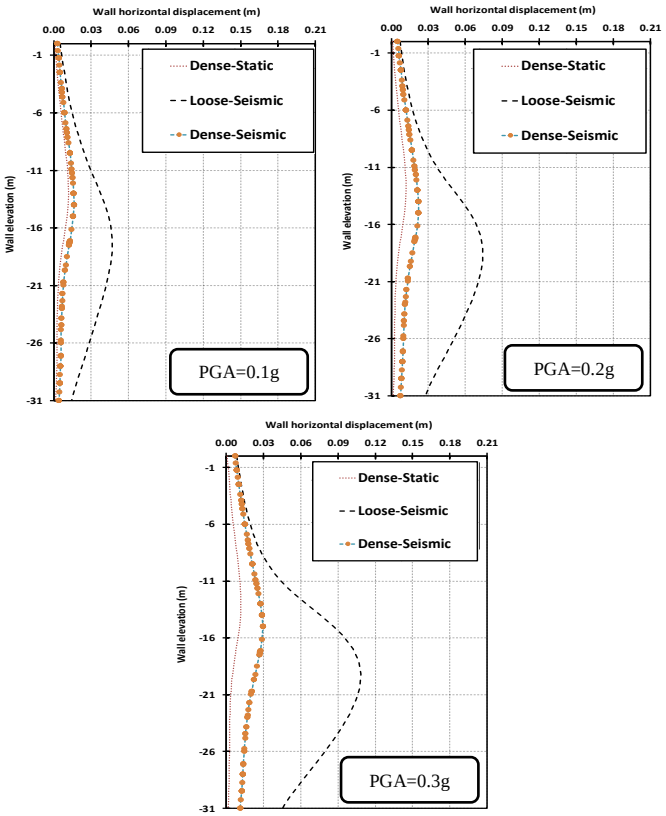

Fig. 4. Plot of wall displacement profiles of dense sand under static condition against range of wall displacements expected to occur under seismic condition (PGA=0.1 to 0.3g),(L/B = 1, H = 15 m)

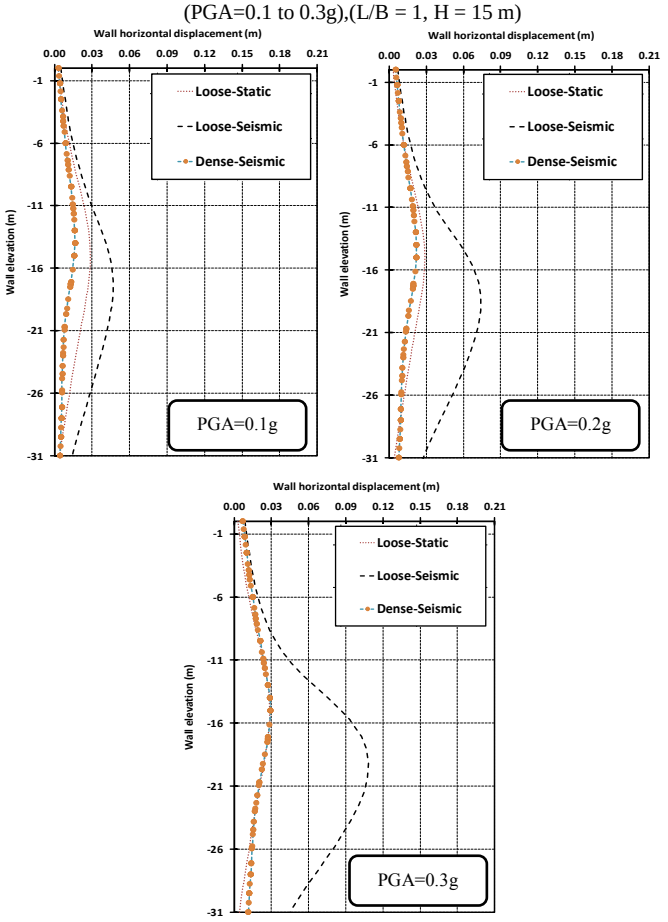

Fig. 5. Plot of wall displacement profiles of loose sand under static condition against range of wall displacements expected to occur under seismic condition (PGA=0.1 to 0.3g) , (L/B = 1, H = 15 m)

For length over width ratio (L/B = 1) of the excavation dimensions on plan, Figure (6) illustrates a series of profiles showing the ground surface movements behind wall of dense sand under static condition against range of ground movements expected to occur under different seismic conditions (PGA=0.1 to 0.3g).

Accordingly, Figure (7) has a series of profiles showing the ground surface movements behind wall of loose sand under static condition against range of ground movements expected to occur under different seismic conditions (PGA=0.1 to 0.3g). Under static condition, the maximum vertical displacements of ground surface are approximately ranging between 0.0061 m and 0.0144 m for dense and loose sands. Under seismic condition, the maximum ground surface displacements are in the range of 0.0118 m and 0.1312 m for peak ground acceleration (PGA) ranging between 0.1 and 0.3g. The maximum vertical displacements of ground surface occur approximately at distance of about 5 m and 17.7 m away from the wall (i.e. at 0.33 to 1.18 H).

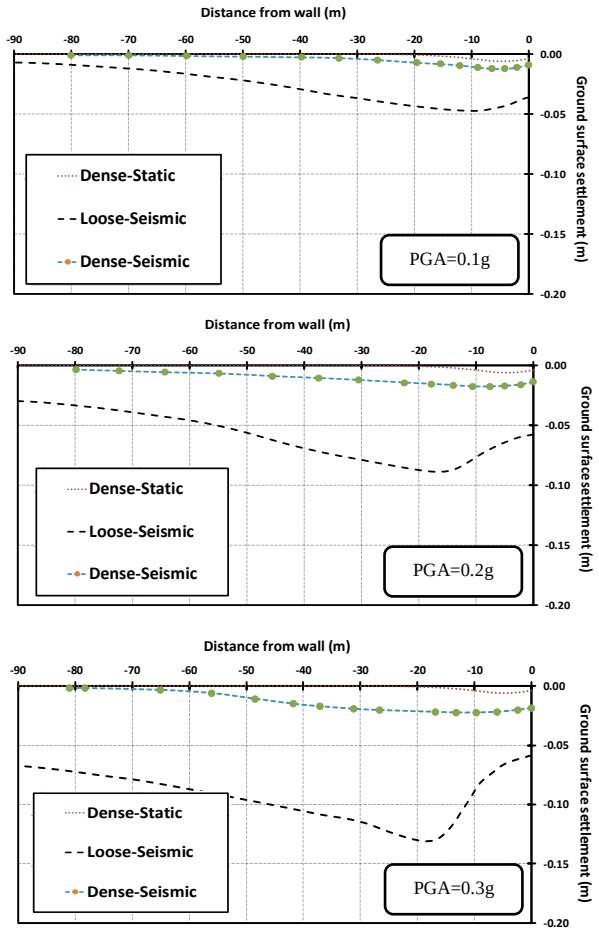

Fig. 6. Plot of ground surface settlements profiles of dense sand under static condition against range of ground settlements expected to occur under seismic condition (PGA=0.1 to 0.3g), (L/B=1, H=15 m)

International Journal of Engineering Research & Technology (IJERT)
ISSN: 2278-0181
Vol. 6 Issue 09, September - 2017

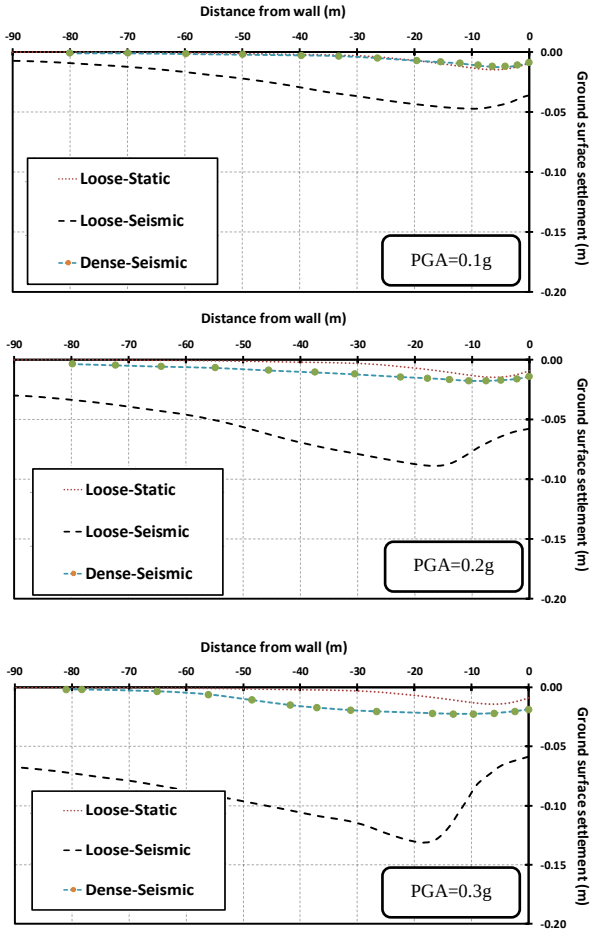

Fig. 7. Plot of ground surface settlements profiles of loose sand under static condition against range of ground settlements expected to occur under seismic condition (PGA=0.1 to 0.3g), (L/B=1, H=15m)

A.2 For Length Over Width Ratio of the Excavation Dimensions on Plan (L/B = 3)

Figure (8) and Figure (9) are illustrating the wall displacement profiles under static and seismic conditions for length over width ratio (L/B = 3) of the excavation dimensions on plan. For the static condition, the maximum lateral displacements of the wall are in the range of 0.0159 m and 0.0657 m for dense and loose sands. For the seismic condition, the maximum wall displacements are within 0.0211 m and 0.1906 m for peak ground acceleration (PGA) oscillating between 0.1 and 0.3g. The maximum wall lateral displacements occur at a depth of around 13 to 16.1 m below ground surface for the static condition, while it is at 14 to 19.8 m for the seismic condition.

For length over width ratio (L/B = 3) of the excavation dimensions on plan, Figure (10) presents a series of profiles showing the ground surface movements behind wall of dense sands under static condition against range of ground movements expected to occur under different seismic conditions (PGA=0.1 to 0.3g). Accordingly, Figure (11) shows a series of profiles showing the ground surface movements behind wall of loose sands under static condition against range of ground movements expected to occur under different seismic conditions (PGA=0.1 to 0.3g). Under static condition, the maximum vertical displacements of ground surface are approximately ranging between 0.0102 m and 0.0376 m for dense and loose sands. Under seismic condition, the maximum ground surface displacements are within 0.0143 m and 0.1321 m for peak ground acceleration (PGA) oscillating between 0.1 and 0.3g. The maximum vertical displacements of ground surface occur approximately at distance of about 0.37 to 1.3 (H) away from the wall.

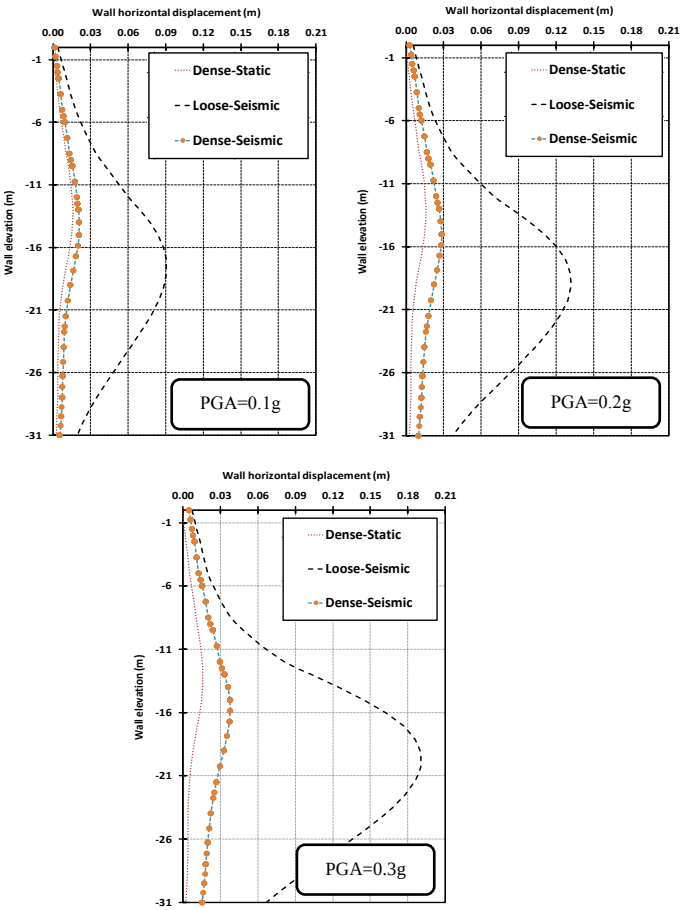

Fig. 8. Plot of wall displacement profiles of dense sand under static condition against range of wall displacements expected to occur under seismic condition (PGA=0.1 to 0.3g),(L/B = 3, H = 15 m)

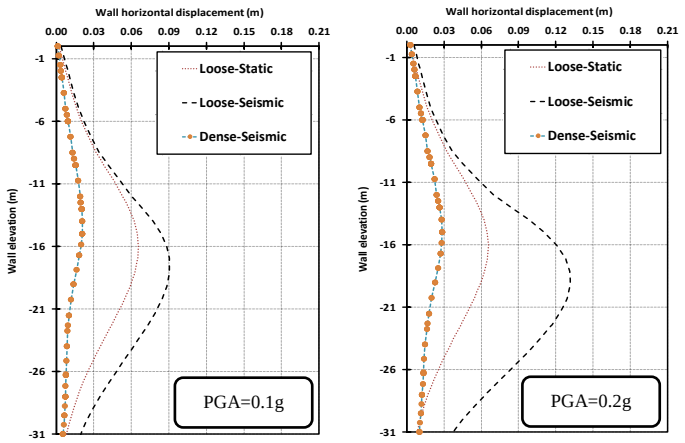

International Journal of Engineering Research & Technology (IJERT)
ISSN: 2278-0181
Vol. 6 Issue 09, September - 2017

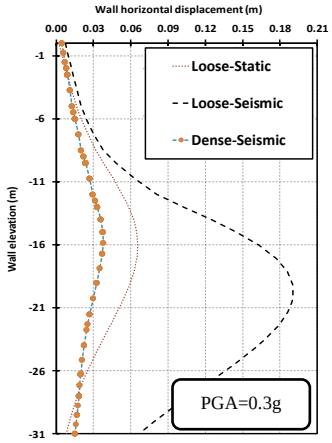

Fig. 9. Plot of wall displacement profiles of loose sand under static condition against range of wall displacements expected to occur under seismic condition (PGA=0.1 to 0.3g),(L/B = 3, H = 15 m)

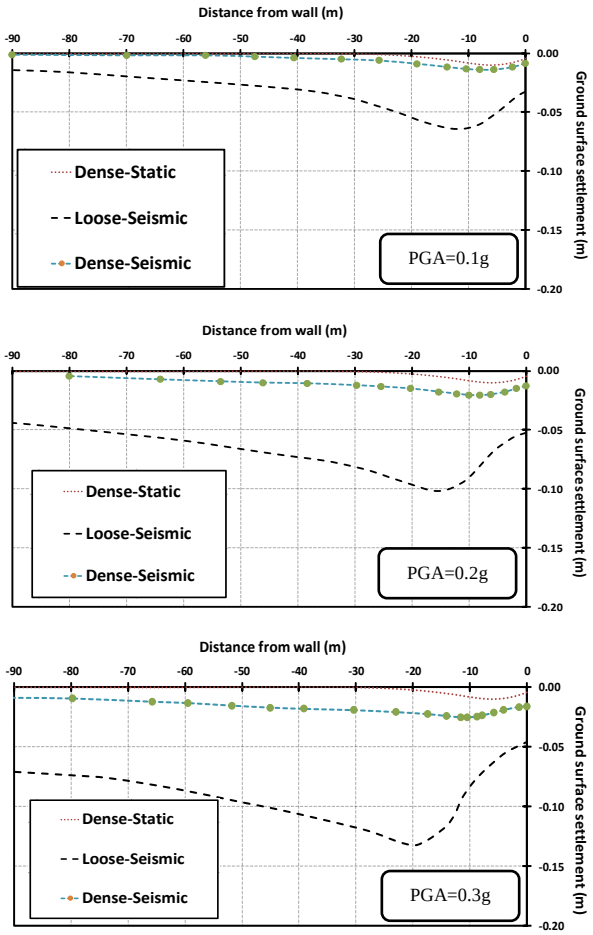

Fig. 10. Plot of ground surface settlements profiles of dense sand under static condition against range of ground settlements expected to occur under seismic condition (PGA=0.1 to 0.3g), (L/B=3, H=15m)

A.3 For Length Over Width Ratio of the Excavation Dimensions on Plan (L/B = 5)

Figure (12) and Figure (13) show the wall displacement profiles under static and seismic conditions for length over width ratio (L/B = 5) of the excavation dimensions on plan. At the static condition, the maximum lateral displacements of the wall are within 0.016 m and 0.067 m for dense and loose sands. At the seismic condition, the maximum wall displacements are in the range of 0.0212 m and 0.196 m for peak ground acceleration (PGA) ranging between 0.1g and 0.3g. The maximum wall lateral displacements occur at a depth of around 13 to 16.3 m for the static condition, and at depth of 14 to 20 m for the seismic condition.

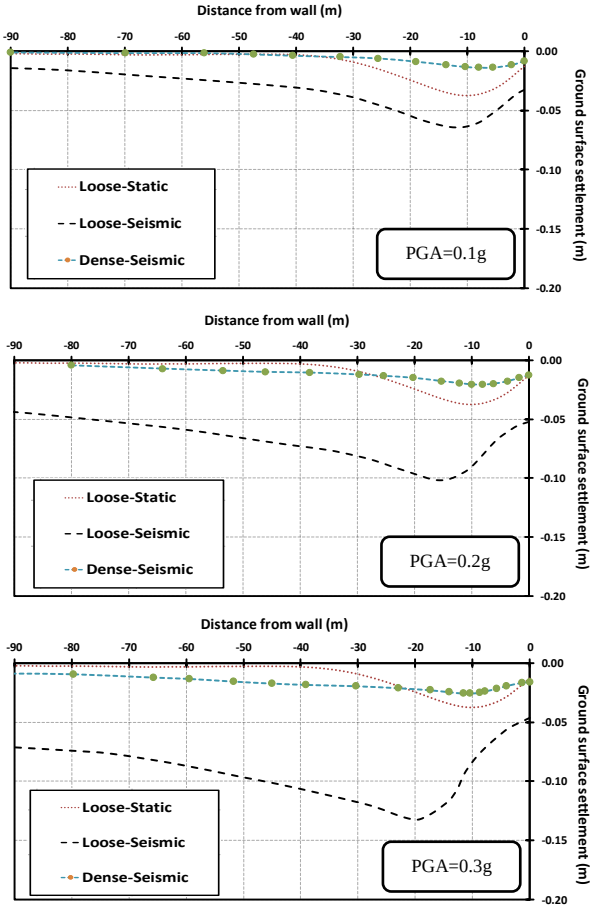

Fig. 11. Plot of ground surface settlements profiles of loose sand under static condition against range of ground settlements expected to occur under seismic condition (PGA=0.1 to 0.3g), (L/B=3, H=15m)

For length over width ratio (L/B = 5) of the excavation dimensions on plan, Figure (14) demonstrates a series of profiles showing the ground surface movements behind wall of dense sands under static condition against range of ground movements expected to occur under different seismic conditions (PGA=0.1 to 0.3g). Accordingly, Figure (15) has a series of profiles showing the ground surface movements behind wall of loose sands under static condition against range of ground movements expected to occur under different seismic conditions (PGA=0.1 to 0.3g). Under static condition, the maximum vertical displacements of ground surface are approximately in the range of 0.0102 m and 0.0386 m for dense and loose sands. However, under seismic condition, the maximum ground surface settlements are ranging between 0.0146 m and 0.1329 m for peak ground acceleration (PGA) oscillating between 0.1 and 0.3g. The maximum vertical displacement of ground surface occur at distance of approximately 0.42 to 1.3 (H) away from the wall.

In light of the previous results, it is noticed that the wall and ground surface movements are increased by enlarging the length over width ratio (L/B) of the excavation dimensions on plan. Moreover, changing the length over width ratio from (L/B

International Journal of Engineering Research & Technology (IJERT)
ISSN: 2278-0181
Vol. 6 Issue 09, September - 2017

= 1 to L/B = 3) has more pronouncing influence on the wall and ground surface movements than varying the length over width ratio from (L/B = 3 to L/B = 5). Changing of the length over width ratio (L/B) of the excavation dimensions on plan has practically no substantial effect on the location of either the maximum wall lateral displacement or the maximum ground surface settlement.

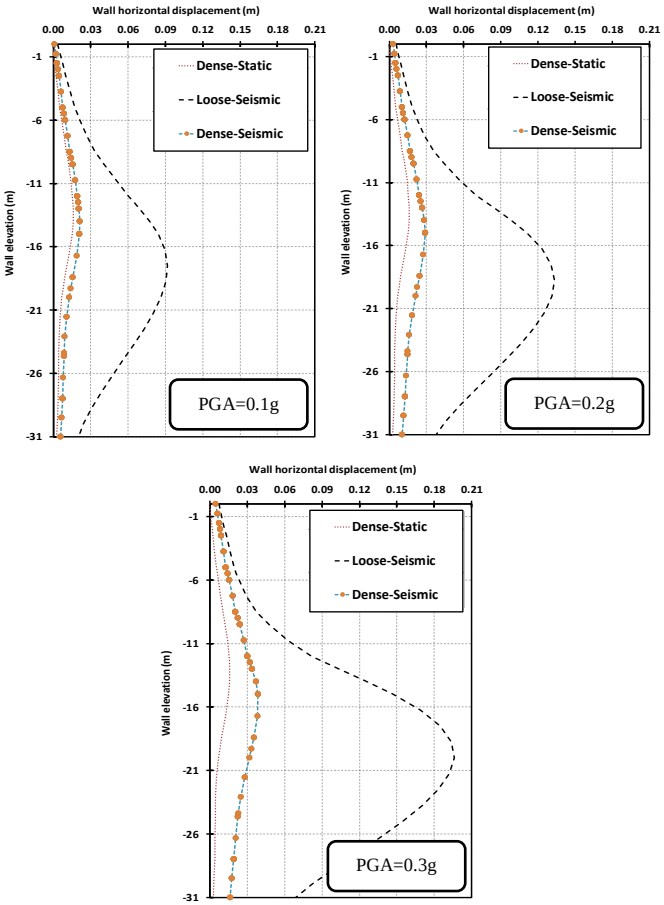

Fig. 12. Plot of wall displacement profiles of dense sand under static condition against range of wall displacements expected to occur under seismic condition (PGA=0.1 to 0.3g),(L/B = 5, H = 15 m)

Figure (16) presents the distribution of maximum lateral wall displacements along the wall for the current case (H=15 m). The wall deformations increase with increasing distance from the corner, however, there is a stationary point where the deformations are no longer increasing, which indicates that the corner stiffening effect is minimized beyond a certain distance from the corner. For loose sand, this stationary point is approximately at 30 m away from the corner (60% of half the wall length), while it is about 18 m away from the corner (36% of half the wall length) for dense sand. This finding is in relatively good agreement with Ahmad et al' [5] who studied the three-dimensional performance for one of Greater Cairo underground metro stations (Rod El-Farag Station), and reported that the three-dimensional corner effects extend to 30% of half the wall length.

It is concluded that as the soil stiffness increases, the corner stiffening effect decreases, and accordingly the stationary point becomes more close to the wall corner

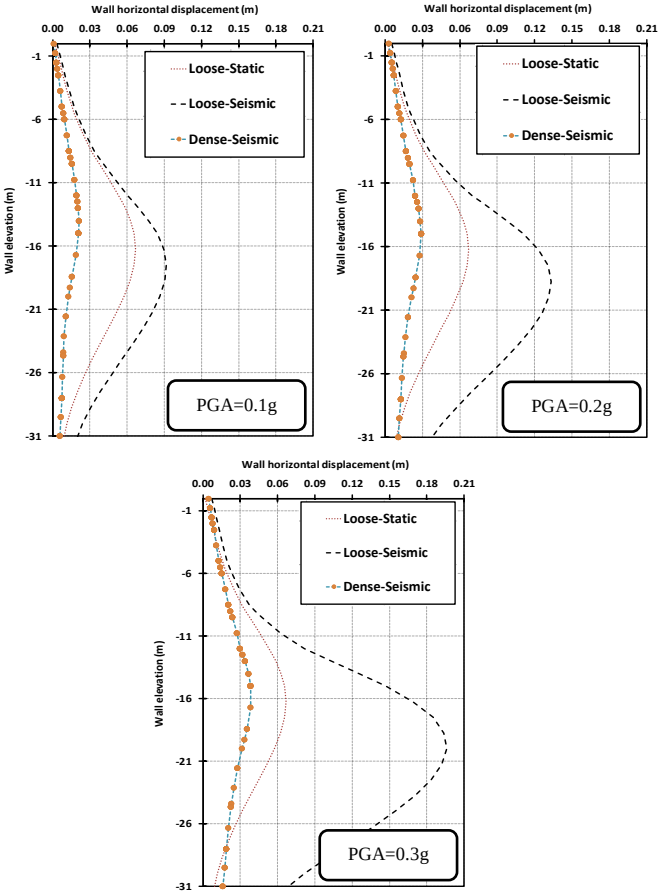

Fig. 13. Plot of wall displacement profiles of loose sand under static condition against range of wall displacements expected to occur under seismic condition (PGA=0.1 to 0.3g),(L/B = 5, H = 15 m)

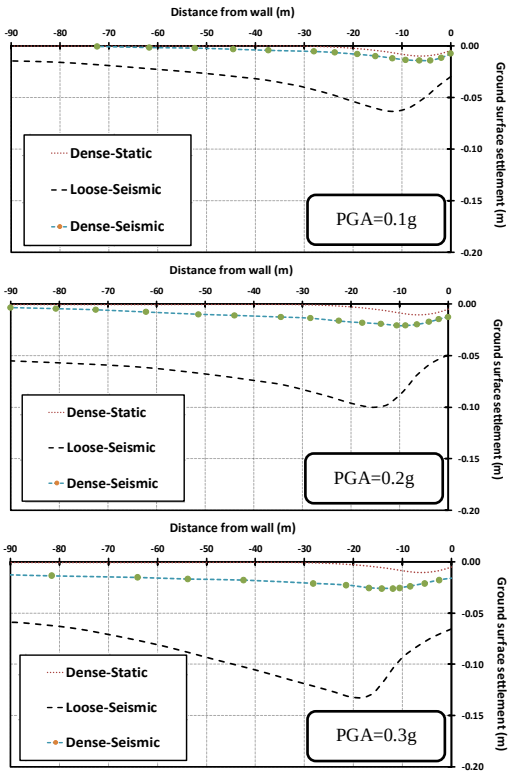

Fig. 14. Plot of ground surface settlements profiles of dense sand under static condition against range of ground settlements expected to occur under seismic condition (PGA=0.1 to 0.3g),(L/B=5, H=15m)

International Journal of Engineering Research & Technology (IJERT)
ISSN: 2278-0181
Vol. 6 Issue 09, September - 2017

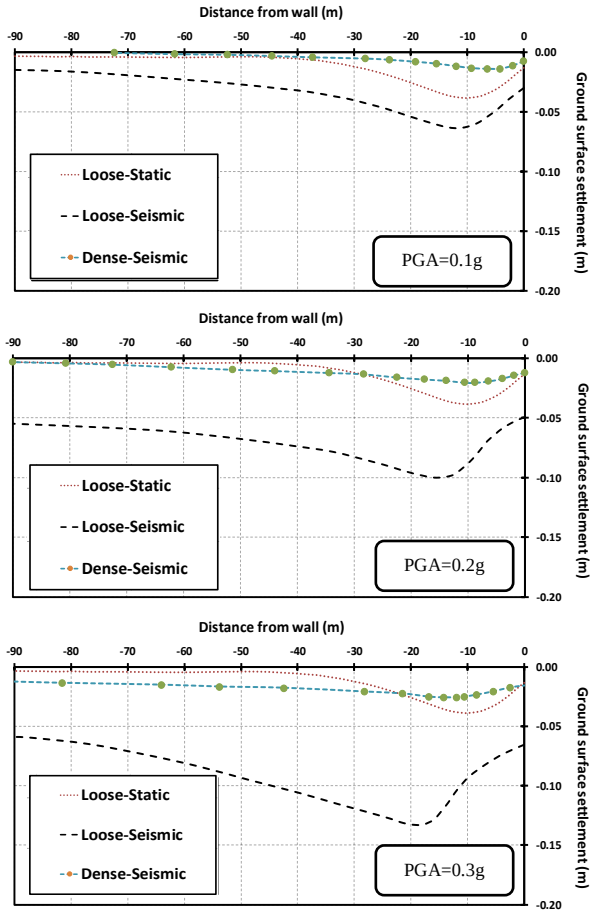

Fig. 15. Plot of ground surface settlements profiles of loose sand under static condition against range of ground settlements expected to occur under seismic condition (PGA=0.1 to 0.3g), (L/B=5, H=15m)

III. NORMALIZED SUMMARY CHARTS

Figure (17) and (18) illustrate the maximum normalized lateral wall displacements and ground surface settlements of different excavation heights (H= 10, 15 & 20 m) for cohesionless soil deposits under static condition against range of wall & ground surface displacements expected to occur under different seismic conditions (PGA=0.1 to 0.3g). The maximum normalized lateral wall displacements (as % of excavation height) are in the average of 0.34% & 0.1% for the static condition, 0.49% & 0.14% for PGA=0.1g, 0.72% & 0.19% for PGA=0.2g, and 1.05% & 0.25% for PGA=0.3g.

The maximum normalized ground surface settlements (as % of excavation height) are in the average of 0.21% & 0.06% for the static condition, 0.40% & 0.09% for PGA=0.1g, 0.66% & 0.12% for PGA=0.2g, and 0.96% & 0.17% for PGA=0.3g.

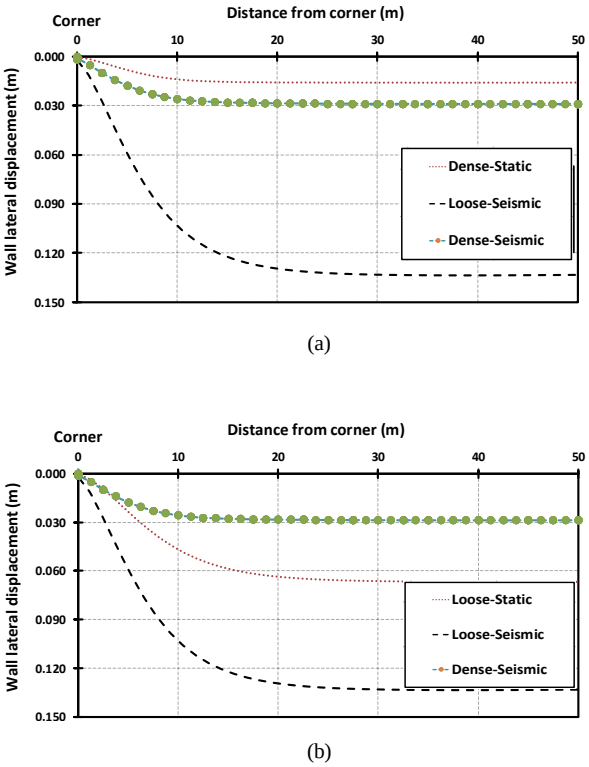

Fig. 16. Distribution of maximum lateral displacements along the wall: (a) dense sand under static condition against range of wall displacements expected to occur under seismic condition (PGA=0.2g); (b) loose sand under static condition against range of wall displacements expected to occur under seismic condition (PGA=0.2g)

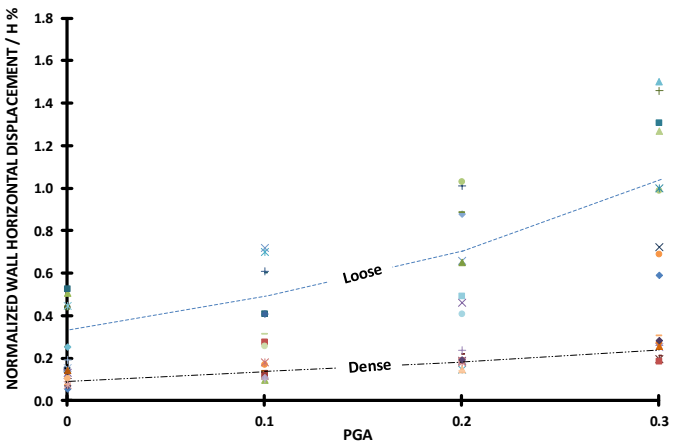

Fig. 17. Plot of the maximum normalized lateral wall displacements of different excavation heights (H= 10, 15 & 20 m) for cohesionless soil deposits under static condition against range of wall displacements expected to occur under different seismic conditions (PGA=0.1 to 0.3g)

International Journal of Engineering Research & Technology (IJERT)
ISSN: 2278-0181
Vol. 6 Issue 09, September - 2017

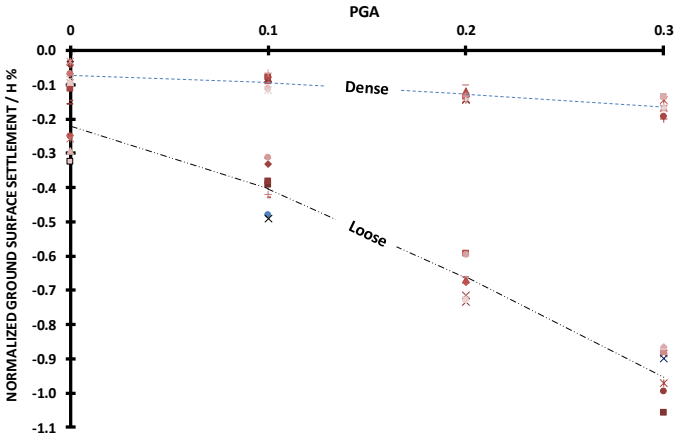

Fig. 18. Plot of the maximum normalized ground surface settlements (behind wall) of different excavation heights (H= 10, 15 & 20 m) for cohesionless soil deposits under static condition against range of ground surface settlements expected to occur under different seismic conditions (PGA=0.1 to 0.3g).

IV. CONCLUSIONS

The main conclusions of the current research work are presented as follow:

a) Reducing the length over width ratio (L/B) of the excavation dimensions on plan causes decreasing the wall and ground surface movements due to the stiffening effects of the corner. However, for length over width ratio greater than 3 (L/B > 3), the stiffening effects of the corner has practically insignificant impact on the movements of the retaining wall and the surrounding soil.

b) The higher of soil stiffness, the lesser of the corner stiffening influence.

c) The wall deformations increase with increasing distance from the corner, even so, the corner stiffening effect is minimized beyond a certain distance from the corner. For loose sand, this distance is approximately 30 m away from the corner (60% of half the wall length), while it is about 18 m away from the corner (36% of half the wall length) for dense sand. This finding is in relatively good agreement with Ahmad et al' [5] who reported that the three-dimensional corner effects extend to 30% of half the wall length.

d) Changing the length over width ratio from L/B = 1 to L/B = 5 has an average increase of approximately 70 % on the maximum wall lateral displacements, while it has an average increase of about 40 % on the maximum ground surface settlements behind wall.

e) The variation of the length over width ratio (L/B) of the excavation dimensions on plan has insignificant effect on the location of both the maximum displacements of the wall and the ground surface.

f) Wide range of wall and ground surface movements shall be expected when the seismic condition is considered, since it has a substantial influence on the wall and ground surface deformations.

REFERENCES

[1] Peck, R.B. (1969), "Deep excavations and tunneling in soft ground". Proceedings of the 7th International Conference on Soil Mechanics and Foundation Engineering, Mexico City, State of the Art Vol. 3.

[2] Goldberg, D.T., Jaworski, W.E.; and Gordon, M.D. (1976), "Lateral support systems and underpinning". Report FHWA-RD-75-128, Vol. 1, Federal Highway Administration, Washington D.C.

[3] Clough, G.W.; and O'Rourke, T. D. (1990), "Construction induced movements of in-situ walls". Design and Performance of Earth Retaining Structures, ASCE Geotechnical Special Publications 25.

[4] Law, K.H.; Roslan, H.; and Zubaidah, I. (2014), "3D numerical analysis and performance of deep excavations in Kenny Hill formation". Proceedings of the 8th European Conference on Numerical Methods in Geotechnical Engineering, Delft, The Netherlands.

[5] Ahmad, A.A.; Hefny, A.M.; Mansour, M.F.; and Mansour M.M. (2015), "Three-dimensional analysis of Rod El-Farag subway station, Greater Cairo Metro". Proceedings of the 14th International Conference on Structural and Geotechnical Engineering, Cairo, Vol. 10.

[6] Wood, J.H. (1973), "Earthquake induced soil pressures on structures". PhD Thesis, California Institute of Technology, Pasadena, CA.

[7] Kitsis, V.G.; Vlachakis, V.S.; Athanasopoulos, G.A.; and Athanasopoulos-Zekkos, A. (2015), "Seismic thrust vs. wall inertia in non-yielding retaining walls under earthquake loading: synchronous or asynchronous action". Proceedings of the International Foundations Congress and Equipment Expo, ASCE Geotechnical Special Publications 256.

[8] Brinkgreve, R.B.J.; Kumarswamy, S.; and Swolfs, W.M. (2015), "PLAXIS: finite element code for soil and rock analyses, reference manual".

[9] Seed, H. B.; Tokimatsu, K.; Harder, L. F.; and Chung, R. M. (1984), "The influence of SPT procedures in soil liquefaction resistance evaluation". Report No. EERC-84/15, Earthquake Engineering Research Institute, University of California, Berkeley, California.